Batteries & Supercaps

Review
doi.org/10.1002/batt.202400811

Chemistry Europe
European Chemical Societies Publishing

www.batteries-supercaps.org

Electrolyte Strategies at Extreme Temperatures for Aqueous Zinc Batteries

Xingtai Liu,[a] Jia Yao,[a] Chao Xia,[a] Xiaofang Wang,[a] Lin Lv,[a] Jun Zhang,*[a] Houzhao Wan,[a] and Hao Wang*[a]

The state of aqueous zinc batteries at extreme temperature environment is an important parameter for their widespread application. However, low ionic conductivity and sluggish ionic diffusion at low temperature, and aggravated untoward reactions in the interface of electrode-electrolyte at high temperature, seriously limit the practical application of zinc-ion batteries. Currently, numerous zinc-ion batteries capable of operating within a broad temperature range have been proposed. Herein, the reason of the performance decline at extreme temperature is discussed from the perspective of thermodynamics and dynamics. Then, from the additives/co-solvents, high concentration salts, hydrogels and other aspects, the main strategies of electrolyte are introduced in detail. Finally, the possible directions to further improve the high and low temperature performance of zinc-ion batteries are proposed. It is hoped that this review will be helpful to the design and manufacture of wide temperature zinc-ion battery electrolyte and provide reference for the application of rechargeable zinc-ion battery in extreme environment.

1. Introduction

With the rapid consumption of conventional energy sources, the development and utilization of renewable energy have become an urgent and crucial research topic to meet the demand of sustainable development.[1] However, the application of these energy sources is subject to many limitations, such as high cost, unstable supply and demand, and harsh storage conditions. Secondary batteries have become one of the most promising energy storage methods due to their high energy density and recyclability, which are of great significance for the sustainable development of human society.[2] The advantages of zinc metal anodes are their low electrochemical potential (compared to the standard hydrogen electrode, it is −0.76 V), high specific capacity (820 mAh g^{-1}) and low cost.[3] Therefore, aqueous zinc-ion batteries (ZIBs) in the field of large energy storage showed a broad appeal.[4] However, due to the limitation of water molecules in the electrolyte, the freezing temperature of conventional electrolytes is often higher at standard atmospheric pressure.[5] At low temperature, ionic conductivity and ionic diffusion rate will be greatly reduced, hindering ion transport. High temperatures can cause irreversible damage to the battery. For example, the cathode material dissolves in the electrolyte and irreversible structural collapse, corrosion of zinc anodes, hydrogen evolution processes, etc. Nevertheless, as human activities expand, the demand for battery operation under extreme environmental conditions is also increasingly high. For instance, exploration in polar regions, near the equator, deserts, aerospace applications, and high-altitude areas necessitates zinc ion batteries that can operate normally under extreme temperature conditions.[6]

To achieve low-temperature operation of ZIBs, two challenges must be addressed: reducing the freezing point (T_f) of the electrolyte and avoiding a sharp drop in ionic conductivity and ion diffusion rate. For ZIBs to operate in high-temperature environments, issues of stability must be resolved, as high temperatures can accelerate zinc anode corrosion, electrolyte decomposition, impacting batteries normal functioning.[7] Generally, there are three recognized approaches to broaden the temperature range of the electrolyte:[8] (i) Using electrolyte additives or co-solvents instead of conventional aqueous-based electrolytes. (ii) Increasing the concentration of zinc salts in the electrolyte, such as water in salt (WIS) strategies. (iii) Utilizing water-based gel electrolytes to broaden the operating temperature of the cell.[9] Recent research on organic additives is a viable approach. By leveraging the various advantages of water and organic substances, mixed liquid electrolytes like Dimethyl sulfoxide (DMSO)[10] and Triethyl phosphate (TEP)[11] demonstrate excellent performance not only in low-temperature and high-temperature environments but also play a significant role in stabilizing the interface between electrode and electrolyte. Chen et al. designed a 7.5 m zinc chloride electrolyte. The role of anions in the electrolyte significantly reduced the T_f.[12] Additionally, ethylene glycol, serving as a co-solvent combined with $Zn(BF_4)_2$ electrolyte, facilitates the in-situ formation of a beneficial ZnF_2 protective layer on the zinc anode, expanding the working temperature range to −30 °C to 40 °C. Although significant achievements have been made in the research of high-temperature and low-temperature electrolytes, a comprehensive summary of the design principles for these electrolytes is still lacking.

In recent years, research on zinc-ion battery electrolytes has made significant progress, underscoring its importance. In this

[a] X. Liu, J. Yao, C. Xia, X. Wang, L. Lv, J. Zhang, H. Wan, H. Wang
Hubei Key Laboratory of Micro-Nanoelectronic Materials and Devices, School of Microelectronics, Hubei University, Wuhan, 430062, PR China
E-mail: gwen_zhang@126.com
nanoguy@126.com
wangh@hubu.edu.cn

review, we elucidate the intrinsic relationship between dynamics and thermodynamics, revealing the fundamental principles behind temperature as a cause of battery failure. We will thoroughly discuss and analyze the research progress of the main strategies, including concentrated electrolytes with high salt content, organic additives/co-solvents, hydrogel electrolytes and organic solvent based non-aqueous solution electrolytes (Figure 1).

2. The Connection Between Dynamics and Thermodynamics

In order to understand the impact of ambient temperature on ZIBs, the influence of extreme temperature conditions on the thermodynamics and kinetics of ZIBs was studied..[13] Voltage is the most intuitive performance of the zinc-ion battery operating parameters, its expression is:

$$E = E_{\emptyset} - \frac{RT}{nF} \ln Q \tag{1}$$

In this formula, E represents the battery operating voltage at ambient temperature, $E_{\emptyset}$stands for the voltage at standard conditions, R is the gas constant, n is the number of electron transfers, and F is Faraday's constant and T is the ambient temperature. Generally, the energy is generated by the electrochemical reaction inside the battery, and the output voltage of the battery conforms to Nernst equation.[14] When a battery is in a state of discharging, $Q < 1$, $\ln Q < 0$; $\frac{RT}{nF} \ln Q > 0$. Hence, as the ambient temperature T decreases, the lnQ will also decrease, and eventually the actual voltage E will decrease. In other words, changes in the operating temperature of the battery will lead to changes in the discharge voltage of the battery, and lead to changes in energy and power density.

From a thermodynamic perspective, increased polarization of the battery at high or low temperatures also leads to voltage losses.[15]

The electrochemical kinetics of a battery are closely intertwined with electrode polarization, encompassing electrochemical polarization (η_a), ohmic polarization (η_0), and concentration polarization (η_c).[8c,16] Here, I is the power current, Ri is the impedance of the battery. The relationship between the working voltage E of the battery and I, Ri and polarization is expressed as:

$$E = E_0 \pm \eta_t \pm IR_i \tag{2}$$

$$\eta_t = \eta_c \pm \eta_a \pm \eta_0 \tag{3}$$

In the equation, the symbols "+" and "-" respectively represent the charging process and discharging process of the battery. The parameters (η_0, ηa and ηc) are affected by a combination of dynamics and thermodynamics.[17] From the formula, it is evident that the battery voltage is influenced by both polarization and internal resistance.[18] Furthermore, these factors are further constrained by temperature.[2b] Figure 2 shows the relationship between dynamics, thermodynamics, and polarization.

Prof. Hao Wang is currently a full professor of the School of Microelectronics at Hubei University, China. He received his BSc in 1989 and his PhD in 1994 from Huazhong University of Science and Technology, China. He joined Hubei University in 2002. He spent several years as a visiting professor at several prestigious institutions, including the French National Center for Scientific Research (CNRS), the Max Planck Institute for Solid State Research, the Royal Institute of Technology (KTH), Aalto University, The Chinese University of Hong Kong, and National Sun Yat-sen University. His current research interests include integrated circuits and new materials for renewable energy.

Prof. Houzhao Wan is currently a full professor at the School of Microelectronics, Hubei University, China. He obtained his PhD degree from Huazhong University of Science and Technology in 2015. He joined Hubei University in 2015. He has published over 60 papers as the first or corresponding author and was listed in the 2020 and 2022 global top 2% scientists list by Stanford University. His current research interests include metal batteries, compound semiconductors, and optoelectronic detectors.

Prof. Jun Zhang is currently a professor at the School of Microelectronics, Hubei University, China. She received her MSc in condensed matter physics from the Institute of Solid State Physics, Chinese Academy of Sciences, in 2003, and her PhD from the University of Salford, UK, in 2007. She joined Hubei University in 2007. In 2015, she worked as a visiting scholar at Aalto University, Finland. Her current research interests include new energy materials and devices (such as solar cells and optoelectronic detectors), and perovskite memory devices.

Dr. Xingtai Liu obtained his Master's degree in Engineering from Hubei University in 2024 and is currently pursuing further studies at the School of Materials Science and Engineering, Beihang University. His research interests include the design of electrolytes for aqueous secondary zinc batteries and the development of halide-based solid-state electrolytes.

Review
doi.org/10.1002/batt.202400811
Chemistry Europe
European Chemical Societies Publishing

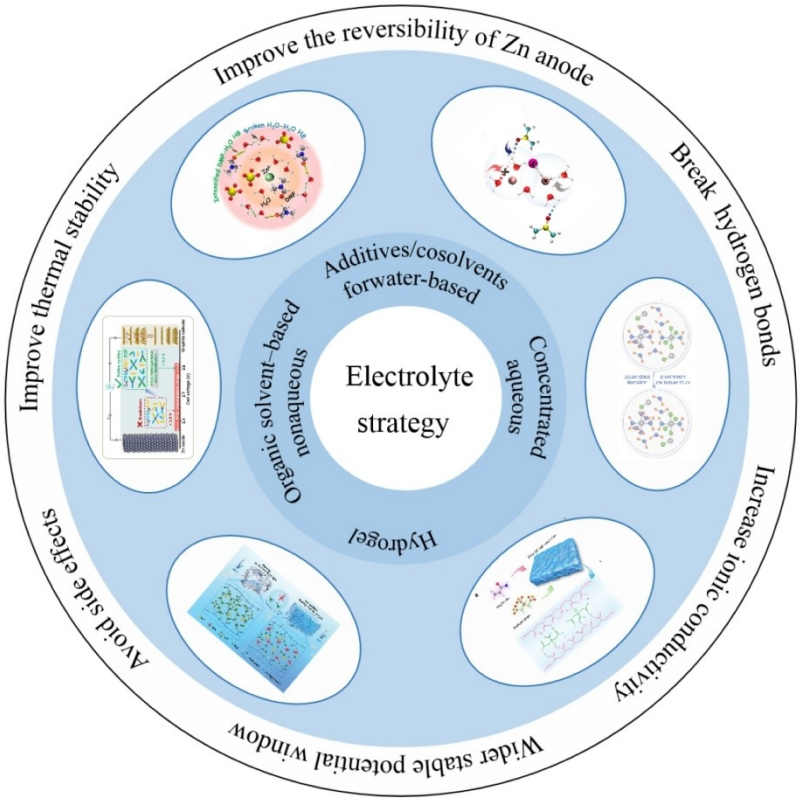

Figure 1. Overview of classification of electrolyte protection strategies for ZIBs at extreme temperature.

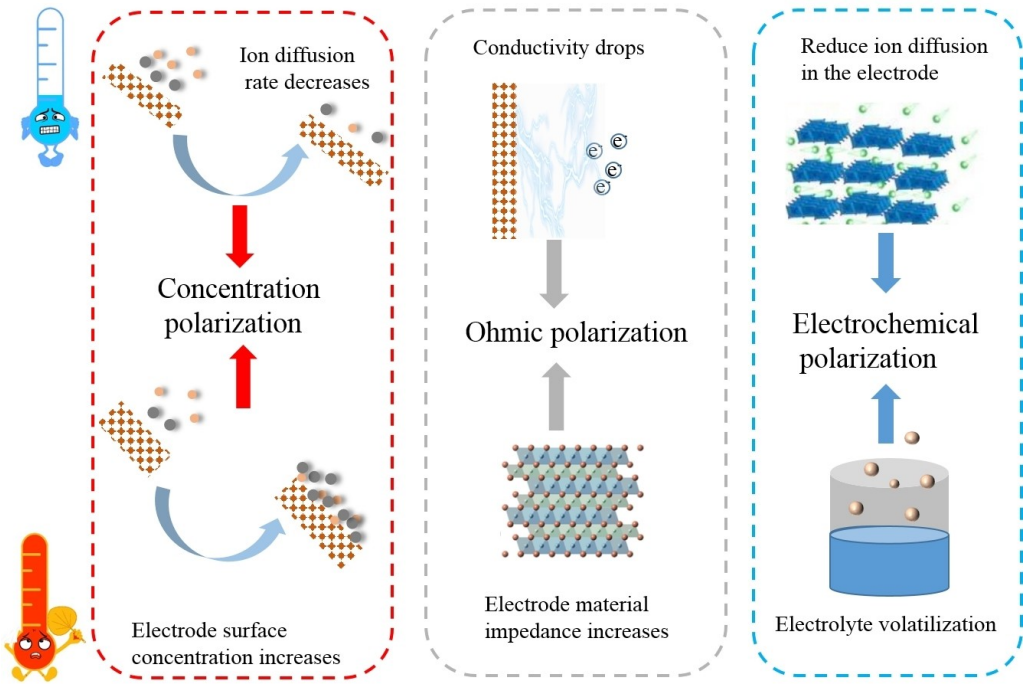

Figure 2. Schematic diagram of battery polarization.

At high temperatures, the ion migration rate increases, which can reduce internal resistance. However, the accelerated reaction kinetics may also lead to rapid chemical reactions, increasing polarization. During charge and discharge processes, intensified interfacial reactions between the electrode and electrolyte, as well as electrode material expansion, can disrupt

the stability of the electrode-electrolyte interface, resulting in greater voltage polarization.At low temperatures, the migration rate of Zn^{2+}ions decreases significantly, and the viscosity of the electrolyte increases. This can lead to a larger potential difference on the battery surface, creating greater polarization and negatively impacting the voltage and power output of the battery.To address these challenges, optimizing the electrolyte is an effective strategy to enhance the performance of aqueous batteries under extreme environmental conditions.

3. Mechanisms and Challenges at Extreme Temperature

In aqueous-based electrolytes, water molecules tend to freeze at low temperatures. This phenomenon significantly inhibits ionic conductivity and interfacial dynamics, resulting in ZIBs unable to work properly at low temperatures.[19] Additionally, the cycling stability of ZIBs is often limited by the slow diffusion rates of ions, irreversible crystalline structural changes in cathode materials, collapse, anode corrosion, dendrite formation, and interface passivation.[20] Compared to organic solvents, water has a higher T_f. Research have shown that the ionic conductivity in the environment below 0 °C will significantly decrease, resulting in an increase in electrode polarization. This is due to a large increase in the charge transfer impedance, resulting in a slower ion transport rate.[21] Furthermore, water undergoes a significant phase transition below 0 °C, accompanied by the phenomenon of salt precipitation in the electrolyte. When the temperature significantly decreases, the precipitated zinc salts hinder ion transfer, reducing the stability window of the electrolyte and impacting the battery's performance.

The challenges faced by zinc-ion batteries differ at high temperatures compared to low temperatures. Compared to lithium-ion batteries, they exhibit excellent safety characteristics at high temperatures due to their inherent advantages.[22] However, at extremely high temperatures, unnecessary side reactions will occur between the electrode liquid and the electrode, which may cause serious corrosion of the zinc electrode, and the increase in temperature will further aggravate this process. At high temperatures, the hydrogen evolution reaction will intensify, increasing the internal pressure of the battery, causing the battery to expand or even break.[23] Therefore, the thermal stability of electrolyte is improved and avoiding side reactions is advantageous to the cells work stable at high temperatures.[24] The failure of batteries using organic electrolytes at high temperatures is usually attributed to thermal runaway. Operating in a high temperature environment, if the surface heat dissipation of the battery is poor, resulting in local overheating, the battery life will be further reduced.[25] More critically, continuous exposure to high temperatures can potentially trigger an explosion.

4. Electrolyte Strategies at Extreme Temperatures

Adjusting electrolyte composition has been shown to be an effective way for batteries to operate at extreme temperatures. In the past few years, experts have made a lot of exploration on widening the operating temperature range of ZIBs, such as introducing organic solvents in conventional electrolytes, designing hydrogel electrolytes, etc.[26] This section will analyze the fundamental principles behind different electrolyte strategies.

4.1. Additives/Co-Solvents

The operating temperature of aqueous-based electrolytes is limited by their high T_f. In contrast, organic solvents exhibit a lower T_f. Adding organic solvents in the electrolyte can be changed in the electrolyte hydrogen bonding, lowering the solid-liquid loading temperature of the electrolyte and improving the thermal stability at high temperatures.[24] Therefore, substituting water with organic solvents that have low freezing points and high flash points as the electrolyte is a feasible approach, such as N, N-Dimethylformamide (DMF),[27] Acetonitrile (AN),[28] Ethylene Glycol (EG),[29] and γ-Butyrolactone (GBL).[30] This approach not only improves the battery's performance under extreme temperature conditions but also ensures the stability and safety of the electrolyte.[31]

EG is commonly used to make antifreeze and has a low melting point.[32] Moreover, it exhibits excellent solubility in water, making it a classic antifreeze agent. Methanol (MeOH) is an organic solvent with high dielectric constant, which has significant advantages in breaking hydrogen bonds (HBs) and improving low temperature performance. EG molecules have hydroxyl groups at both ends, causing HBs to form between the molecules. This creates long chains of EG, akin to a "hand-in-hand", which limits the electrolyte's low-temperature properties. These long EG molecular chains were broken by adding 40% MeOH (Figure 3a).[29a] In addition, even at −50 °C, the electrolyte with added MeOH does not freeze, which greatly expands the temperature range of the electrolyte.

Organic solvents containing electron-rich functional groups exhibit a strong affinity for zinc, allowing them to modulate the Zn^{2+} internal solvation sheath and improve the stability of zinc anode (Figure 3b).[15c,28b,31,33] Acetamide, with its abundant electron-donating functional groups ((C=O) and -NH_2), was introduced as an additive alongside short-chain Acetamide and long-chain silk amino acids in a aqueous-based electrolyte (referred to as DE-AS), enhancing broad-temperature adaptability and interface stability (Figure 3b). In the DE-AS electrolyte, the zincophilic molecule acetamide can enter the internal solvation sheath of Zn^{2+}, replacing some of the water molecules in the solvation sheath. Acetamide can reconstruct the hydrogen bond network in the electrolyte, significantly reducing the proportion of strong HBs (as shown in Figure 3c), and increasing the proportion of weak HBs. At an ambient temperature of

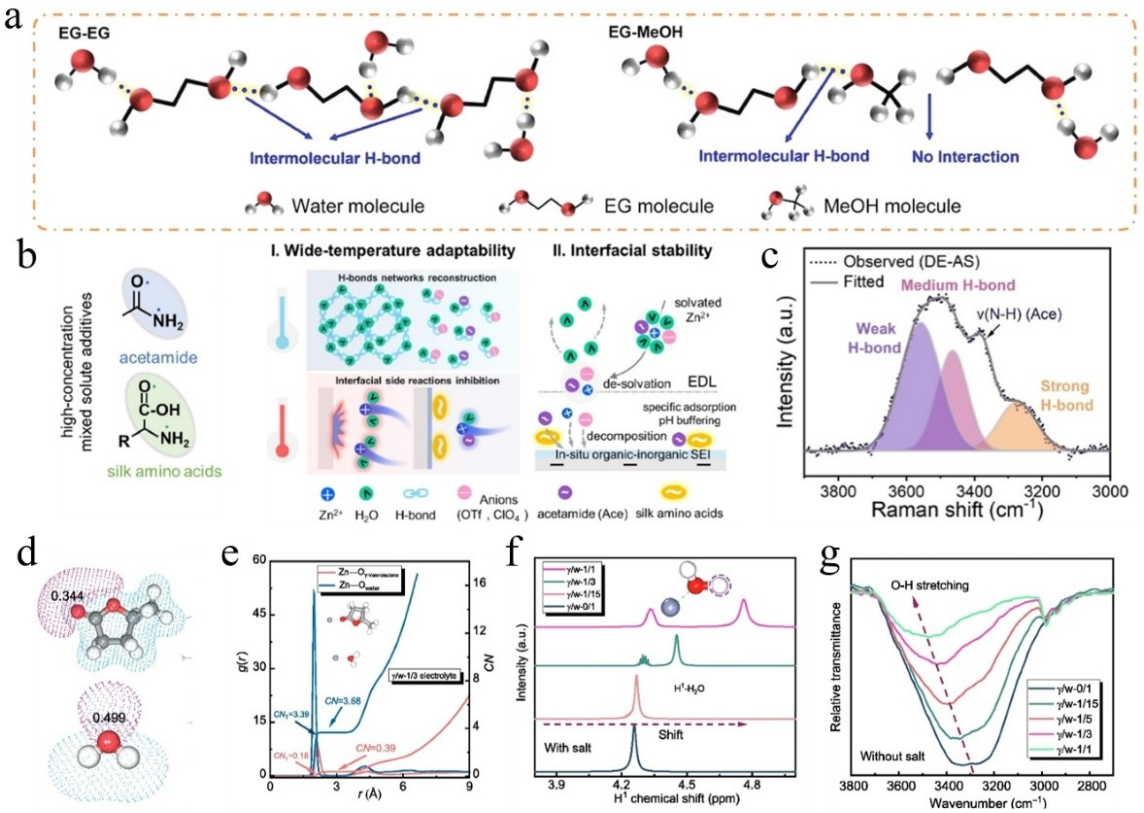

Figure 3. Additives/co-solvents break hydrogenbond networks to improve ZIBs performance in extreme environments. (a) Schematic diagram of MeOH breaking EG-EG intermolecular forces. (Reproduced with permission.[29a] Copyright 2023 Wiley-VCH). (b) Schematic of the main mechanisms of acetamide and silk amino acids in electrolytes and interfaces. (c) Raman spectra of strong, medium and weak HBs in DE-AS electrolyte. (d) The electron density distribution of water molecular and c-valerolactone molecular. (Reproduced with permission.[33] Copyright 2023 Elsevier B.V.). (e) The RDFs of Zn^{2+}-solvent of c/w-1/3 hybrid electrolyte. (f) ^{1}H Magnetic Resonance (NMR) spectra of the c-valerolactone electrolytes. (g) Fourier Transform Infrared Spectroscopy (FTIR) of the c-valerolactone electrolytes. (Reproduced with permission.[34] Copyright 2023 Elsevier B.V.).

60 °C, a full battery assembled with DE-AS can maintain 75% capacity after 100 cycles at a current of 1 A g^{-1}.

Most organic solvents in the electrolyte as additives or co-solvents can enter the internal solvation sheath of Zn^{2+}, replacing some of the solvation sheath water molecules. Some weak solvent molecules do not enter the internal solvation sheath of Zn^{2+}, but instead form a weak solvation effect, facilitating the coordination between zinc ions and water molecules, thereby confining the water molecules within the solvation sheath..[35] γ-valerolactone is a weak solvent molecule with a low steric hindrance effect (Figure 3d) and a weak coordination charge density with zinc-oxygen.[34] The radial distribution functions showed that γ-valerolactone hardly enter the internal solvation sheath of Zn^{2+} (Figure 3e). The mechanism of γ-valerolactone in the electrolyte was investigated by ^{1}H Nuclear NMR and Fourier Transform Infrared Spectroscopy (FTIR). As shown in Figure 3f and 3 g, with the increasing of γ-valerolactone content, the lower the frequency shift of the O–H bond of electrolyte, indicating that the new HBs are formed between γ-valerolactone and water molecules. These HBs break the strong HBs between H_2O and H_2O and reduce the T_f of the electrolyte. Zn||PANI batteries using this electrolyte show stable cycling performance at both −30 °C and 30 °C temperatures

In addition to changing the solvation structure of Zn^{2+},[36] additives/co-solvents can also protect zinc anode by inducing uniform deposition of zinc ions on the zinc surface,[37] avoid the problems of zinc dendrites and corrosion caused by extreme temperature environments,[38] and improve the cycle life of zinc ion batteries in high and low temperature environments.[26b,39] Li et al.[53] designed a unique solvation structure with MeOH as an additive. When a certain amount of MeOH was added to the electrolyte, the inner solvation sheath of Zn^{2+} will become $Zn(H_2O)_2(CH_3OH)_2^{2+}$ (Figure 4a). This unique solvated structure repels active water from the interface between the electrode and the electrolyte, and during the cycle, both MeOH and $Zn(CF_3SO_3)_2$ decompose, forming an organic and inorganic hybrid SEI on the zinc surface, avoiding the corrosion and hydrogen evolution reactions that occur in zinc anodes at high temperatures.[40]

Adjusting the orientation of 2D Zn^{2+} deposition can also avoid the side reaction of zinc negative electrode in extreme environment.[37a] Betaine (Bet) is a kind of common security, non-toxic, alkaloid, it can with the water molecules to form HBs in the electrolyte, the activity of lower free water in the

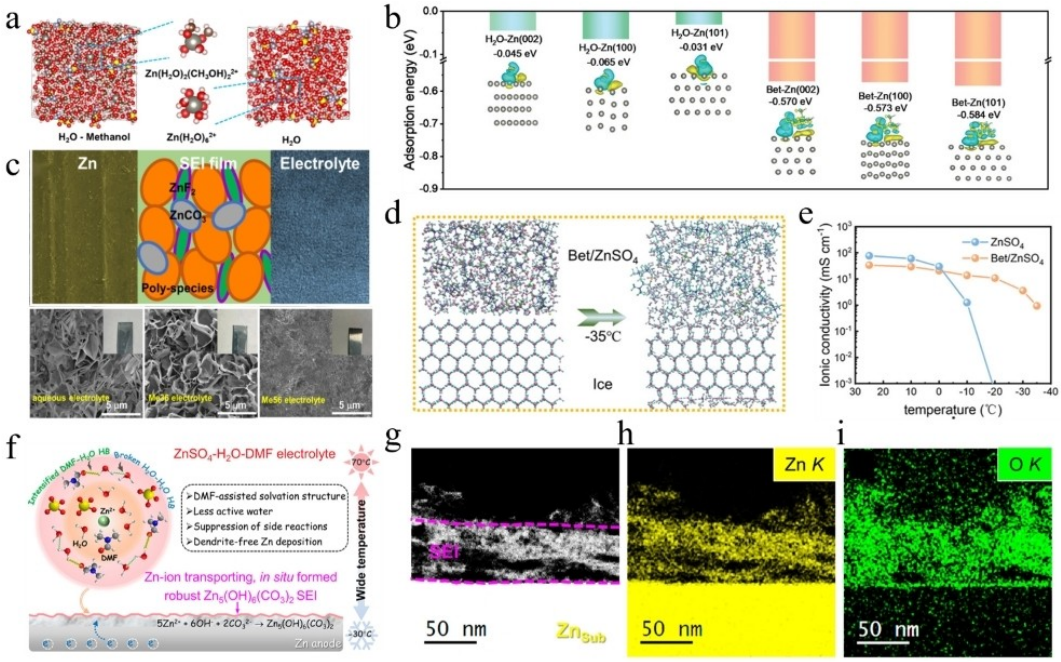

Figure 4. Additive/co-solvent stabilized zinc anode to alleviate dendrite and corrosion at extreme temperature. (a) MD snapshot of 1 M $Zn(CF_3SO_3)_2$ in MeOH and aqueous electrolytes. (b) Organic inorganic hybrid SEI stabilizes zinc anode interface. (Reproduced with permission.[40] Copyright 2023 American Chemical Society). (c) Absorption energy comparison of H_2O and Bet molecules on various Zn crystal planes and charge density difference model. (d) Snapshots of 100 ns MM–MD simulations using solid-liquid two-phase model of $ZnSO_4$/Bet electrolyte. (e) Ionic conductivities of Bet/$ZnSO_4$ electrolyte and $ZnSO_4$ electrolyte. (Reproduced with permission.[9] Copyright 2022 Wiley-VCH). (f) Solvation structure and in situ SEI mechanism of $ZnSO_4$-H_2O-DMF electrolyte. (g-i) In situ formed SEI and :Energy Dispersive X-Ray Spectroscopy elemental maps of Zn and O. (Reproduced with permission.[43] Copyright 2023 American Chemical Society).

electrolyte.[41] The adsorption energy of Bet on different crystal faces of zinc is greater than that of water (Figure 4c), indicating that Bet preferentially adsorbs on the surface of zinc anode, regulates two-dimensional Zn^{2+} orientation deposition, and inhibit dendrite growth on zinc anode surface. Adding Bet to the electrolyte can also make the electrolyte withstand lower ambient temperatures Through molecular mechanics (MM–MD) simulation, the ice-liquid interface model was established, and it was found that Bet/$ZnSO_4$ electrolyte also had good freezing resistance at −35 °C (Figure 4d). Compared with aqueous electrolytes, the Bet/$ZnSO_4$ electrolyte ion conductivity is also significantly improved at different temperatures (Figure 4e).[9] Zn-VO_2 full batteries also have excellent cycle stability at −30 °C.

In addition, N, N-dimethylformamide (DMF) is a commonly used organic solvent with high dielectric constant and good solubility, and has been used as an additive for various ion batteries.[42] Zhang et al. modified the solvated structure of Zn^{2+} with water and mixed electrolytes of N, N-dimethylformamide, and in-situ grew a layer of SEI on the surface of Zn (Figure 4f).[27a,43] As a protective layer, the SEI film limits the decomposition of water, avoids the corrosion of the zinc anode by the electrolyte at high temperatures, and provides an ionic conductive layer for uniform Zn^{2+} flux. Zinc-ion capacitors assembled with this electrolyte can cycle stably over a temperature range of −35 °C to 70 °C (Figure 4g–i).

In summary, the use of organic solvents as additives or co-solvents in the electrolyte reduces the interactions between H_2O molecules, reduces the ratio of strong HBs in the electrolyte, thereby improving the ionic conductivity and improving its thermal stability. Additionally, these additives or co-solvents play a stabilizing role at the interface between electrode and electrolyte. They are adsorbed on the electrode surface and act as a uniform electric field, promoting uniform deposition of Zn^{2+} and avoiding problems such as dendrites and corrosion of the zinc anode. Therefore, in future application of organic solvents, it is crucial to consider not only their impact on elevating the working temperature of the electrolyte, but also their protective effect on the zinc anode to enhance its cycling stability.

4.2. Concentrated Electrolytes with High Salt Content

In the electrolyte, increasing the concentration of zinc salts in the water, thereby reducing the T_f of the electrolyte.[37b,44] However, a mere escalation of metal salt concentration is not a prudent course of action.[45] This will impact the physical properties of the solution, intensifying the interaction between zinc ions and anions, consequently resulting in an increase in the viscosity of the solution and a decrease in the conductivity. Therefore, it is imperative to judiciously regulate the concentration of metal salts in the solution.

Cationic and anionic coordination effects can expand the temperature range of electrolyte.[46] A method of adding 3.5 M $Mg(ClO_4)_2$ to 1 M $Zn(ClO_4)_2$ electrolyte has recently been

reported. Mg^{2+} has a smaller ionic radius than Zn^{2+} (Figure 5a-b), and the interaction with O in water is strong, disrupting the existing hydrogen bond network. With the increase of the concentration of zinc perchlorate, the proportion of strong HBs between H_2O and H_2O in the electrolyte decreases, and the synergy of cation and anion in electrolyte electrolyte low temperature resistance was improved greatly (Figure 5c). Zn|| Pyrene-4,5,9, 10-tetraone (PTO) batteries with this electrolyte are capable of stable operation at temperatures of −70 °C with little capacity attenuation.

In addition to cations, the role of anions in high concentration electrolytes can not be ignored. By adjusting the concentration of the zinc chloride electrolyte, the hydrogen bond network (HBs) in the electrolyte can be broken and the T_f of the electrolyte can be reduced. The anions in the $ZnCl_2$ electrolyte have strong interactions with the water molecules, which can break the original HBs (Figure 5d). With the increase of $ZnCl_2$ concentration, the proportion of strong HBs in electrolyte decreased, while the proportion of weak HBs increased. When the concentration of $ZnCl_2$ is 7.5 m, the T_f of electrolyte was the lowes t(−114°C) (Figure 5e).

In electrolytes, anions can also act as hydrogen bond receptors, altering the H-bond between H_2O and H_2O.[49] Fluorine has the highest electronegativity and can cause the fluoroborate anion to exhibit a variety of coordination patterns with water molecules (Figure 5f).[48] BF_4^- can form weak HBs with water molecules, increasing the concentration of $Zn(BF_4)_2$ from 1 M to 4 M, increasing the ratio of OH–F bonds and decreasing the ratio of O–H bonds (Figure 5g). The results show that the interaction between water molecules is weakened, which is conducive to increasing T_f of the electrolyte. T_f of 4 M $Zn(BF_4)_2$ reaches its lowest point, falling to −122.3 °C. Zn|| TCBQ batteries assembled with 4 M $Zn(BF_4)_2$ can also operate stably in extreme environments of −60 °C.

$Zn(TFSI)_2$ has attracted more and more attention due to its excellent ion transport performance. In the $Zn(TFSI)_2$ electrolyte, the number of HBs significantly decreases (Figure. 5 h).[21a] This also suggests that 4 M $Zn(TFSI)_2$ can more effectively reduce the strong HBs in the electrolyte, so that the electrolyte can operate

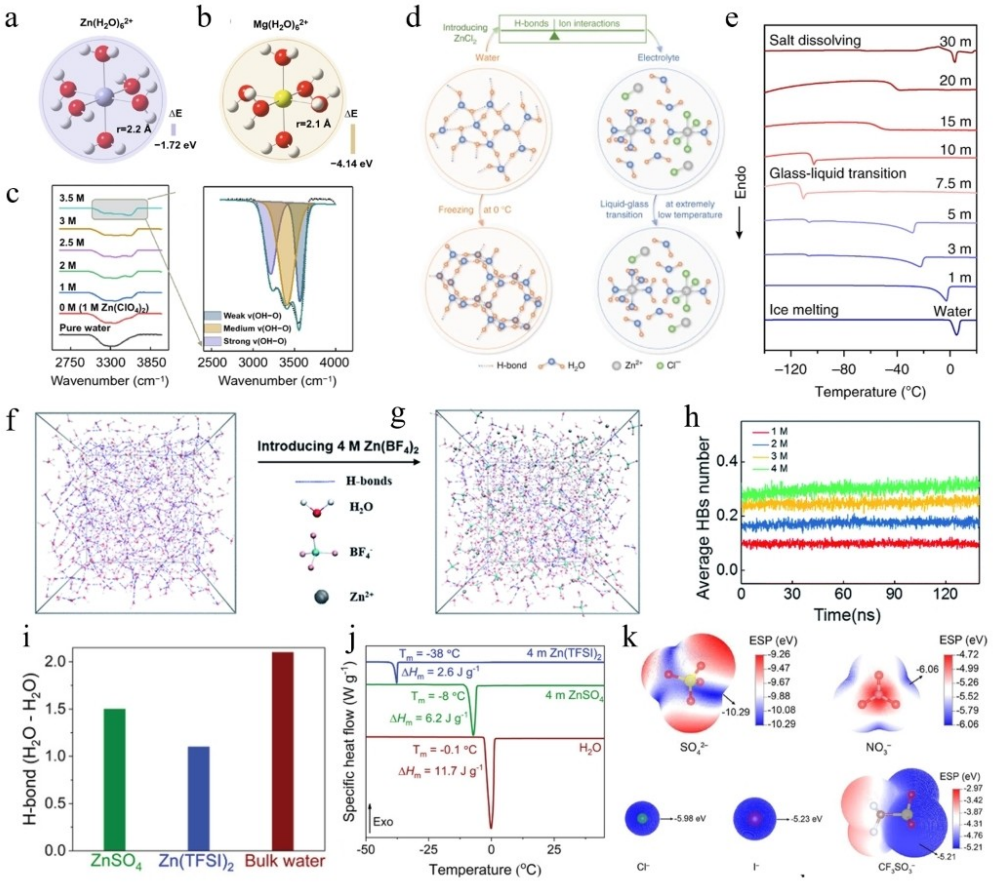

Figure 5. Summary of recent advances on concentrated aqueous electrolytes and the illustration of the mechanism. Formation energy and hydration radius of the solvation structures of (a) Zn^{2+} and (b) Mg^{2+}. (c) FTIR spectra for O–H bond. (Reproduced with permission.[46a] Copyright 2021 Springer Link). (d) Schematic illustration of the structural evolution of water and electrolyte. (e) Differential scanning calorimetry (DSC) test of different concentrations of $CZnCl_2$ from −150 °C to 20 °C. (Reproduced with permission.[47] Copyright 2020 Springer Nature). (f) Snapshot of the MD simulation of $Zn(BF_4)_2$ electrolyte. (g) Average HB numbers for $Zn(BF_4)_2$ electrolyte after 140 ns simulation time. (Reproduced with permission.[48] 2021 The Royal Society of Chemistry). (h) The average number of H-bonds between water molecules in the 4 m $ZnSO_4$, $Zn(TFSI)_2$, and bulk water. (i) differential scanning calorimetry thermograms of 4 m $ZnSO_4$, $Zn(TFSI)_2$, and bulk water. (Reproduced with permission.[21a] Copyright 2021 Wiley-VCH). (j) DFT calculation to obtain ESP values for different anions. (Reproduced with permission.[24] 2022 Elsevier B.V.).

in a wider temperature range. It can be seen the DSC results that T_t of 4 M $Zn(TFSI)_2$ is low (Figure 5i). The $Zn(TFSI)_2$ assembled full battery can operate stably at temperatures of 30 °C and −35 °C.

In summary, thigh concentration of anions in the electrolyte and cations combined, can greatly destroy the original HBs in the electrolyte.[24] Density Functional Theory (DFT) shows that the anions have a lower electrostatic potential (ESP) (Figure 5j), and the H atoms in the electrolyte are more easily combined with the anions than the O atoms, so that the O–H in the electrolyte is destroyed, thereby reducing T_f of the electrolyte. At the same time, while reducing T_f, maintain high conductivity, increase the transfer number of Zn^{2+}, and accelerate the electrolytic reaction. High concentrations of metal zinc salts also have significant advantages in stabilizing the zinc anode interface.

4.3. Hydrogel Electrolyte

Conventional hydrogels tend to solidify at around 0 °C, which limits their use in low-temperature batteries. Elastic hinged hydrogels composed of hydrated polymer chains can effectively lower the T_f. Additionally, hydrogel colloids coated on the surface of the zinc anode can isolate the hydrogel from the external environment, preserving moisture in the electrolyte and preventing water evaporation from the hydrogel. This enhances thermal stability.

Based on different crosslinking agents in hydrogels, they can be classified into two types: chemical crosslinking and physical crosslinking. Physical crosslinking mainly involves in-situ polymerization using polyvinyl alcohol. Chemical crosslinking primarily employs three types of crosslinking agents: polyacrylic acid, polyacrylamide and biopolymer. Water molecules in the hydrogel electrolyte can be divided into three types: free water, weakly bound water and strongly bound water, and the interaction with the hydrogel electrolyte is different. Strongly bound water has stronger interactions with the functional groups in the hydrogel, and the T_t of strongly bound water can be as low as −100 °C. There are three strategies for widening the temperature range of hydrogel electrolytes: (i) Increase the concentration of salts in the solution or add organic solvents. (ii) Change the hydrogel network to enhance the interaction between water molecules and hydrogels. (iii) Coat the surface of the hydrogel with an elastomer to prevent water molecules from migrating to the external environment, thus preventing the evaporation of moisture in the electrolyte.

It is easy to debond between organic molecules and polymer chains in the 3D network of hydrogel electrolytes.[52] Introducing organic solvents into hydrogels through chemical crosslinking is an effective strategy. The hydroxyl group of EG molecule is covalently bound to an isocyanate group, and dimethylhydroxypropionic acid (DMPA) is used as chain extender. Subsequently, the EG-waPUA precursor is copolymerized with acrylamide (AM) to form a novel double-cross-linked hydrogel based on EG-waPUA/PAM (Figure 6a).[50] The use of covalent cross-linked bonds combined with physical HBs greatly improves the flexibility and ductility of hydrogel electrolytes. More than 20% of EG-waPUA hydrogel electrolytes have a low T_f (Figure 6b) and high elasticity (Figure 6c), and the abundant micropores in EG-waPUA matrix hydrogels can be used to transport zinc ions, so that the electrolyte has a high ionic conductivity (Figure 6d).

The concentration and type of zinc metal salts can both affect the gelation point of hydrogels.[53] Using $Zn(BF_4)_2$ and polyacrylamide (PAM) results in excellent low-temperature properties. The F atom in $Zn(BF_4)_2$ is strongly electronegative, and the BF_4^-anion forms OH–F bonds with the water molecule, effectively decreasing the proportion of O–H bonds.[54] In the $Zn(BF_4)_2$-PAM electrolyte, the PAM polymer chain contains abundant charged groups, and this excellent structure can interact with more water molecules. Therefore, the number of HBs in the $Zn(BF_4)_2$-PAM electrolyte is much lower than that in the $ZnSO_4$-PAM electrolyte (Figure 6e). The binding energy of $Zn(BF_4)_2$-PAM-H_2O is lower than that of $ZnSO_4$-PAM-H_2O, indicating that $Zn(BF_4)_2$-PAM-H_2O electrolyte is more stable (Figure 6f). Hence, the $Zn(BF_4)_2$-PAM electrolyte can function at lower temperatures.[51] Flexible ZIBs composed of $Zn(BF_4)_2$-PAM hydrogels can operate stably at −70 °C (Figure 6g).

The conductivity and ductility of with high moisture content are poor at low temperature, resulting in the battery cannot work stably.[55] Wong designed a simple, low-cost hydrogel electrolyte by incorporating cotton into a mixture of tetraethyl orthosilicate and glycerin (Figure 7a).[56] The resulting CT3G30 hydrogel exhibits good conductivity at different temperatures (Figure 7b), and Zn/MnO_2 cells assembled using this hydrogel electrolyte maintain stable cycling over a long period of time in the temperature range of −40 °C to 60 °C. A dual-network hydrogels (CSAM) was synthesized using CMCS and PAM (Figure 7c). The ternary interactions among the ClO_4^- anions, water and and CSAM hydrogel improved the water retention rate of the hydrogel electrolyte and reduced T_f of the electrolyte (Figure 7d).[24] At the same time, at a low temperature of −30 °C, CSAM still has a relatively high elongation rate (Figure 7e).[57]

Zwitterions can adjust the Zn^{2+} coordination environment in the solvation sheath and promote the Zn^{2+} in the orderly deposition on the zinc anode. Yang designed a supramolecular zwitterionic hydrogel electrolyte (SZHE), in which the amphoteric ionic water part creates a water-free environment at the electrode/electrolyte interface. Under an applied electric field, zinc ions can be selectively adsorbed on the surface of the Zn anode, promoting the orderly deposition of Zn^{2+} on the zinc surface (Figure 7f-g). Moreover, the SZHE hydrogel electrolyte water retention is very excellent, and the SZHE hydrogel electrolyte can still maintain more than 90% of the original weight after being exposed to 35–50% of the open air environment for a long time (Figure 7h).[6a]

Increasing the concentration of hydrogel electrolytes is also an effective strategy to enable zinc-ion batteries to operate in extreme environments.[42b,50,58] The $Zn(CF_3SO_3)_2$-PAM electrolyte combines the advantages of hydrogel electrolytes and high concentration electrolytes. It not only possesses the wide operating temperature characteristics of high-concentration

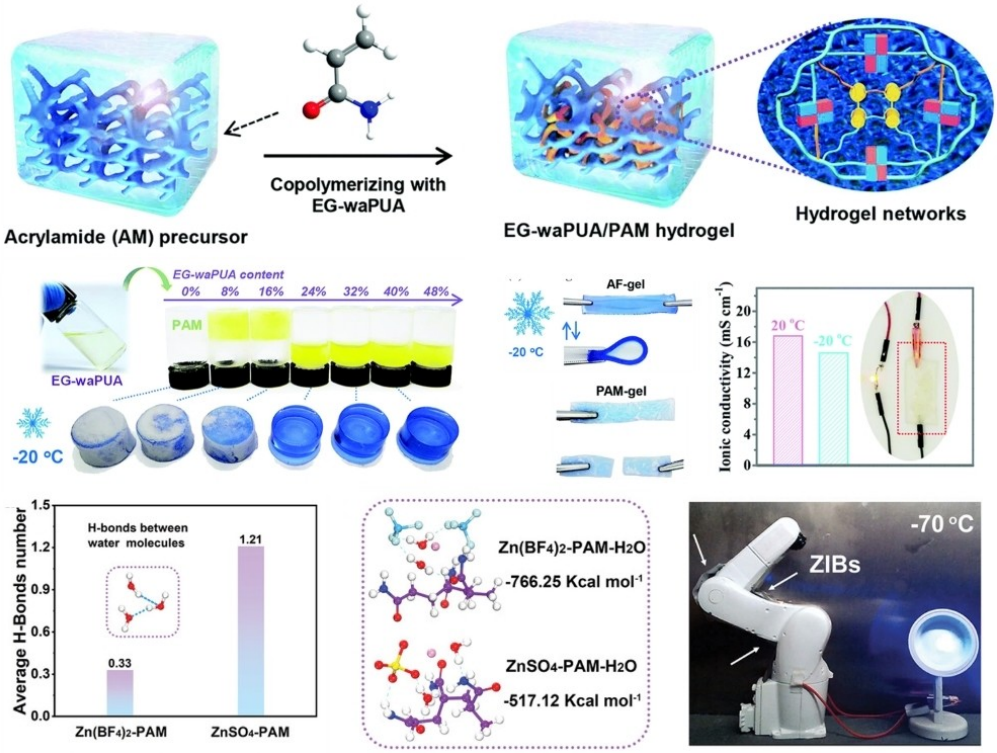

Figure 6. Summary of recent advances on hydrogel electrolytes and the illustration of the mechanism. (a) The synthetic process of EG-waPUA gel. (b) The effect of EG-waPUA weight percentage (Gw%) on the freeze-resistant performance of the hydrogel electrolyte afterone day of cooling at 20 °C. (c) Elastic stability of the AF-gel at 20 °C. (d) Ionic conductivity calculated from AC impedance spectra. (Reproduced with permission.[50] Copyright 2019 The Royal Society of Chemistry). (e) The binding energy of $Zn(BF_4)_2$-PAM-H_2O system and $ZnSO_4$-PAM-H_2O system obtained by DFT simulation. (f) The average number of H-bonds formed between water molecules obtained by MD simulation. (g) Application of batteries composed of $Zn(BF_4)_2$-PAM-H_2O gel electrolyte at −70 °C. (Reproduced with permission.[51] Copyright 2023 Wiley-VCH).

electrolytes but also benefits from the gel electrolyte's ability to suppress dendrite growth and hydrogen evolution.[59] After increasing the concentration, the $Zn(CF_3SO_3)_2$-PAM can widen the operating voltage window.

In summary, the effective methods for expanding the operational temperature range of hydrogel electrolytes, such as using concentrated electrolytes and incorporating electrolyte additives or co-solvent, all work by disrupting the existing hydrogen bond network in the electrolyte. This results in a decrease in the proportion of strong HBs and inhibits the activity of water in the electrolyte..[60] Compared with other electrolytes, hydrogel electrolytes have a three-dimensional network of a large number of charged groups and hydrophilic groups, which can effectively expand the operating temperature of the battery. The charged groups in the hydrogel can improve the ionic conductivity of the electrolyte and promote the transfer of Zn^{2+}. In addition, the hydrogel electrolyte has unique mechanical properties, which makes the electrolyte can be in close contact with the zinc anode, avoid the growth of dendrites, and improve the reversibility of the zinc anode.

4.4. Organic Solvent-Based Nonaqueous Electrolytes

Using organic solvents with higher flash points to completely replace water in the electrolyte is a common method. However, this places high demands on the solubility of the organic solvent. This is because there are few organic solvents that can dissolve zinc salts in the absence of water. Commonly used highly soluble solvents include N, N-dimethylformamide, ethylene glycol, and acetonitrile.[45]

Most organic solvents have difficulty dissolving zinc salt alone, DMF is a very versatile solvent that also exhibits a good ability to dissolve zinc salts. A wide-temperature organic electrolyte was designed using 0.5 M $Zn(OTf)_2$ in DMF, the mechanism of which is shown in Figure 8a. DMF molecules form a complex with Zn^{2+}, increasing the solubility of zinc salts.[61] At the same time, the binding energy between DMF and the Zn anode is high, which facilitates Zn^{2+} uniform deposition, suppresses dendritic growth, and prevents orrosion of the zinc anode. As shown in Figure 8b, ^{1}H NMR also confirmed the chelation of Zn^{2+} with DMF. The Zn//PQ-MCT full battery can operate from −70 °C to 150 °C.

The use of non-combustible organic solvents to prepare pureiy organic electrolytes that are free of water is also an effective method. TEP, a commonly used flame retardant, significantly enhances the non-flammability of the electrolyte

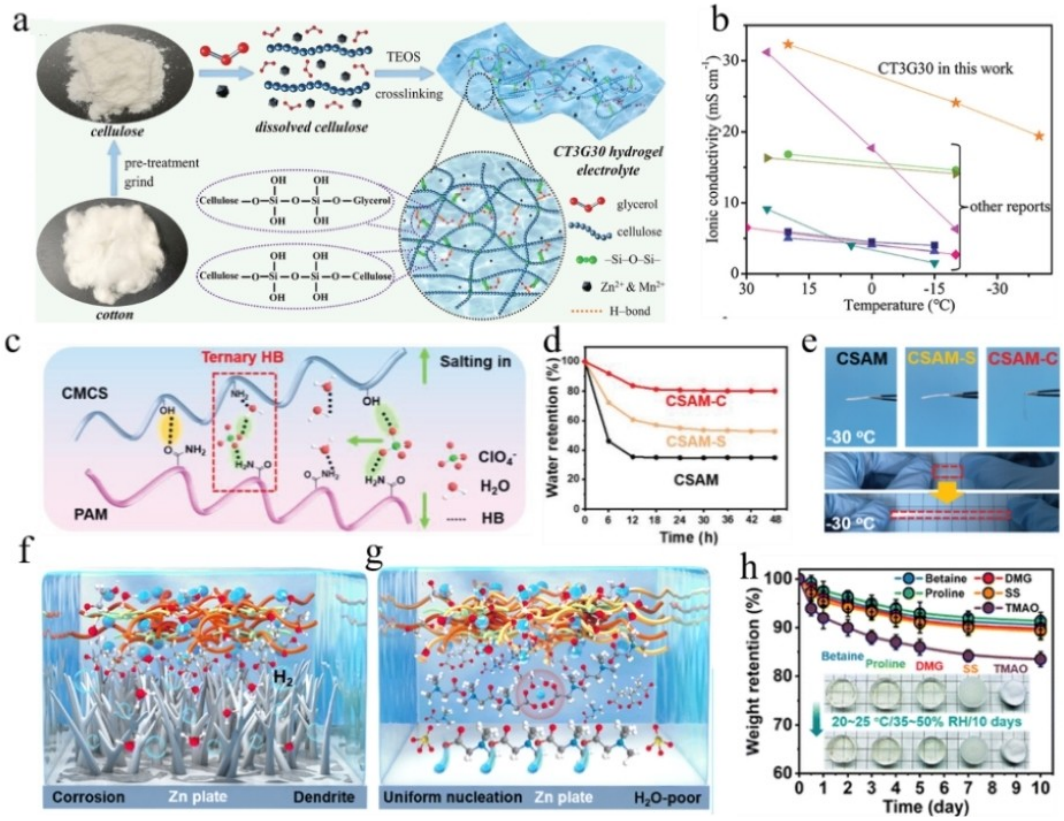

Figure 7. Summary of recent advances on hydrogel electrolytes and the illustration of the mechanism. (a) Schematic illustration of the fabrication of CT3G30 hydrogel electrolyte. (b) Comparison of ionic conductivity of CT3G30 gel electrolyte with other gel electrolytes. (Reproduced with permission.[56] Copyright 2021 Wiley-VCH). (c) Schematic diagram of the interactions among CMCS, ClO_4^-, and PAM chains in CSAM–C hydrogel. (d) Comparison of water retention of different CSAM hydrogel electrolytes. (e) Comparison of the flexibility of CSAM, CSAM–S and CSAM–C hydrogels at low temperatures. (Reproduced with permission.[57] Copyright 2022, Wiley-VCH). Schematic of the Zn^{2+}solvation structure and corresponding deposition behavior in (f) CP/EGZn and (g) CP/EGZn/betaine hydrogel electrolytes. (h) Volatility tests ofthe CP/EGZn/zwitterion hydrogel electrolytes. (Reproduced with permission.[57] Copyright 2022 Wiley-VCH).

when added.[65] The interaction between TEP and Zn^{2+} was stronger, thereby improving the solubility of $Zn(OTf)_2$ in the electrolyte. When Propylene carbonate (PC) is introduced into the electrolyte, the operating temperature of the battery increases to 60 °C with a TEP:PC ratio of 1:2 (Figure 8c).[62] Trimethylolpropane (TMP) is also a commonly used flame retardant. A non-combustible electrolyte was designed by TMP and zinc carbonate, which improved the oxidation stability of zinc carbonate and reduced the side reaction in high temperature environment (Figure 8d).[41a,63]

T_f is one of the most fundamental properties of the electrolytes. MeOH is the simplest monoalcohol, exhibits a significantly lower T_f than that of water (MeOH has a T_f −97.5°C). Zinc chloride is mixed with MeOH and methylene chloride to form a non-flammable electrolyte called WASE. The mechanism of electrolyte was studied by Raman spectroscopy (Figure 8e). The O–H tensile peak is prominent in the Raman displacement spectrum. It is proved that O–H in zinc chloride electrolyte will have strong interaction and destroy the structure of the electrolyte and reduces the T_f of WASE electrolyte to 119.2 °C. WASE electrolyte can avoid the side reaction on zinc surface and enhance the cycling stability of zinc anode. Compared to MeOH and water, the zinc surface remains free of impurities after 100 cycles in the WASE electrolyte, which also maintains its clarity and transparency after cycling (Figure 8e).[64,66]

Compared with additives or co-solvent strategies, pure organic electrolytes are anhydrous, usually have a wider operating temperature range and higher ionic conductivity, and avoid severe hydrogen evolution and corrosion reactions in high temperature environments, which is conducive to improving the thermal stability of zinc-ion batteries. However, pure organic electrolytes have higher requirements for organic solvents. In order to design a pure organic electrolyte that can stably operate at both high and low temperatures, the following conditions must be met: (i) a higher flash point and a lower melting point; (ii) low viscosity; (iii) high solubility for metal zinc salts; (iv) environmentally friendly and pollution-free; (v) low cost. However, the study of most high-concentration electrolytes remains challenging due to the poor solubility of most zinc salts in solvents and the decrease in ionic conductivity caused by high concentrations of electrolytes.

In all, optimizing the electrolyte to reduce T_f and improve the thermal stability remains an effective approach to ensure the stability of the battery in extreme environments. Figure 9a–d compares four different electrolyte strategies from different perspectives. Figure 9e and Table 1 shows the comparison of properties of some electrolytes.

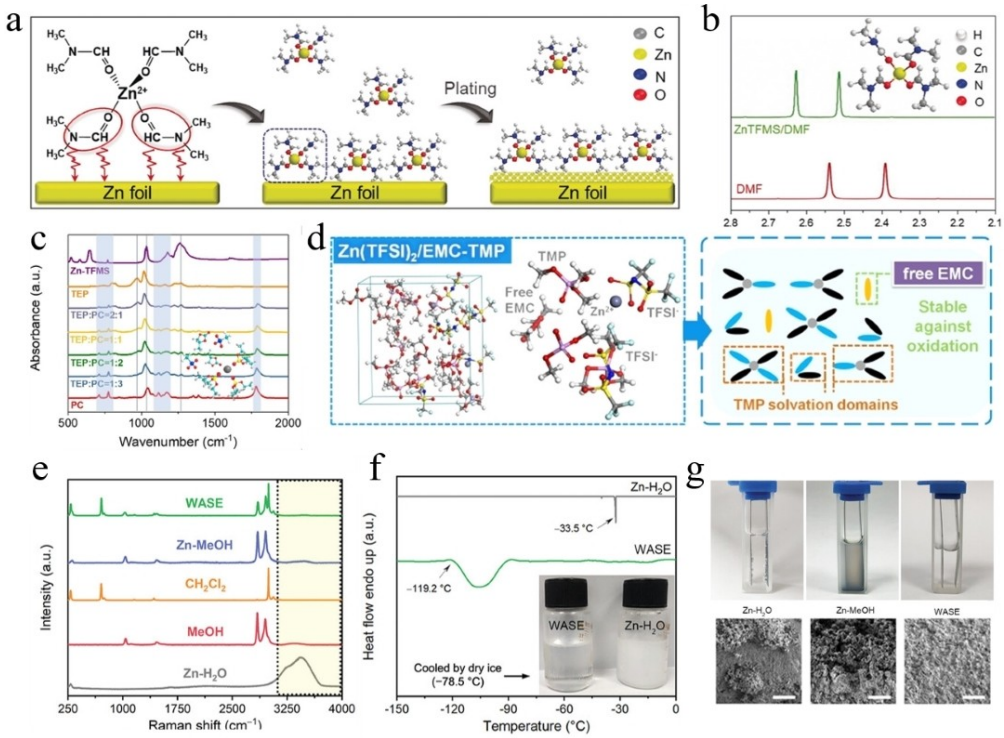

Figure 8. Summary of recent advances on organic solvent–based nonaqueous electrolytes and the illustration of the mechanism. (a) Schematic illustration of Zn^{2+}-DMF complexes facilitate the smooth Zn deposition in ZnTFMS/DMF electrolyte. (b) ^{1}H NMR spectra of pristine DMF and 1.0 mol L^{-1} ZnTFMS/DMF electrolyte. (Reproduced with permission.[61] Copyright 2020 Wiley-VCH). (c) FTIR spectra of Zn-TFMS/(TEP + PC) electrolytes. (Reproduced with permission.[62] Copyright 2020 Wiley-VCH). (d) solvation structures for 1.5 M $Zn(TFSI)_2$/EMC-TMP (1 : 3 by volume). (Reproduced with permission.[63] Copyright 2020 Wiley-VCH). (e). The Raman investigation of WASE, Zn-MeOH, Zn-H_2O, MeOH, and CH_2Cl_2. (f)The Tf of WASE and Zn-H_2O measured by DSC. (g) Photo of WASE electrolyte after circulating in a homemade electrolyzer and SEM of zinc anode surface. (Reproduced with permission.[64] Copyright 2020 Wiley-VCH).

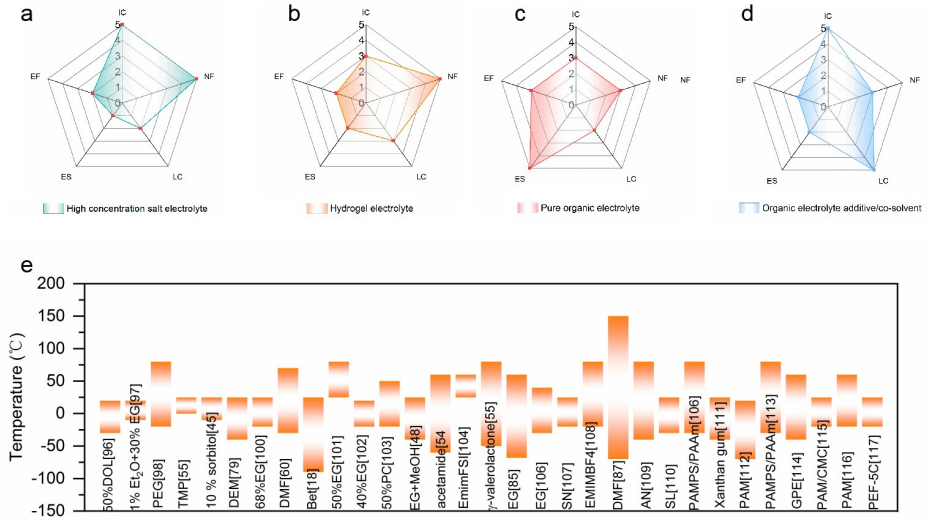

Figure 9. Compare different electrolyte design strategies and some recently reported operating temperature ranges of electrolytes. (a-d) Comparison of different electrolyte design strategies (IC: Ionic conductivity; EF: Environmental friendliness; LC: Low cost; NF: Non-flammability; WS: Electrochemical stability). (e) Operating temperature of partial electrolyte.[9,27a,29a,33–34,39b,44,61,92]

In optimizing the additives/solvent co-solvent strategy for electrolytes, balancing safety and performance is crucial. While organic co-solvents like acetonitrile and dimethyl carbonate significantly improve low-temperature performance, their low flashpoints may pose safety risks. In contrast, organic solvents with low melting points, high flashpoints, and low volatility are considered safer co-solvent options. Moreover, multifunctional additives in electrolytes show great potential; in addition to

Table 1. By electrolyte modification of ZIBs extreme temperatures.

Category	Electrolyte	Cathode	Voltage range	Ionic conductivity ($mS\,cm^{-1}$)	Freezing point (°C)	Operating temperature range (°C)	Ref
Additives/co-solvents	$Zn(BF_4)_2$/EG/MeOH	V_2O_5	0.2–1.6	0.14 (−60 °C)	*	−30–25	[67]
	$Zn(OTf)_2$/$Zn(ClO_{4)2}$/Acetamide/Silk amino acids/H_2O	PANI	0.4–1.5	*	−96	−60–60	[68]
	$Zn(OTf)_2$/γ-valerolactone/H_2O	PANI	0.4–1.5	*	−97	−50–80	[69]
	$Zn(OTf)_2$/DME/H_2O	a-MnO_2	0.2–1.6	1.06(−40 °C)	−52.4	RT–40	[70]
	$ZnSO_4$/DMF/H_2O	AC	0.2–1.8	0.04 (−30 °C)	*	−30–70	[71]
	$ZnSO_4$/Bet/H_2O	VO_2	*	0.935 (−30 °C)	-92	−30–25	[72]
	$Zn(BF_4)_2$/EG/H_2O	VO_2	0.3–1.8	4.5	*	−30–40	[73]
	M $Zn(CF_3SO_3)_2$/DOL/H_2O	V_2O_5·$1.6H_2O$	0.3–1.6	30	−95.3	−30–RT	[74]
Concentrated electrolytes with high salt content	$Zn(BF_4)_2$/H_2O	TCBQ	0.5–1.5	1.47 (−117 °C)	−122	−95–20	[75]
	7.5 m $ZnCl_2$	PANI	0.5–1.5	1.79(−60 °C)	−114	−90–60	[76]
	3 M $Zn(ClO_4)_2$/H_2O	MnO_2	0.8–2	4.23 (−50 °C)	*	−50–20	[77]
	4 m $Zn(TFSI)_2$/H_2O	P(4VC86-stat-SS14)	0.5–2	*	−38	−35–25	[78]
	7.6 m $ZnCl_2$/0.05 m $SnCl_2$	$VOPO_4$	0.2–1.8	0.8 (−70 °C)	−70	−70–20	[79]
	0.4 m $ZnSO_4$ + 2.7 m $Mg(ClO_4)_2$	AC	0.0–2.1	7.5 (60 °C)	−80	−60–RT	[80]
Hydrogel electrolyte	$Zn(BF_4)_2$-PAM	PANI@SWCNTs	0.5–1.5	2.38 (−70 °C)	−117	−70–25	[81]
	$Zn(CH_3COO)_2$/PAA-Na	MnO_2/C	0.5–1.5	0.19 (25 °C)	−57.4	25−−20	[82]
	$ZnCl_2$/NH4Cl/EG/PAMPS/PAM	PANI@SWCNTs	0.5–1.5	1.62 (−30 °C)	< −60	−30–80	[83]
	$Zn(CF_3SO_3)_2$-PAM	$M_{g0.1}V_2O_5$·H_2O	0.1–1.6	27.1 (−20 °C)	*	−30–80	[84]
	$Zn(ClO4)_2$, PAM, DMSO	V_2O_5	0.2–1.7	7.1	−70	−20–80	[85]
	$Zn(ClO4)_2$, PAM, EG	V_2O_5	0.2–1.7	17.2	−60	−40 to 80	[86]
	$Zn(ClO_4)_2$, PAM, Gly	V_2O_5	0.2–1.7	3.6	−20	−20–70	[86]
	$ZnCl_2$/PAM	MnO_2	0–2.2	0.016	< −60	0–60	[86]
	$Zn(TFSI)_2$/EMC/TMP	Graphite	1.4–2.8	*	*	*	[87]
	$Zn(CF_3SO_3)$2/DMF	PQ-MCT	1–1.8	*	*	−70–150 °C	[88]
Organic solvent-based nonaqueous electrolytes.	$ZnCl_2$/MeOH/DCM	PANI	0.3–1.6	2.65 (−50 °C)	−78.5	−78.5–25 °C	[64]
	$Zn(TFSI)_2$/PC/TMP	(PTPAn)	1–2	*	*	*	[89]
	$EMIMBF_4$/TEP	N-doped carbon nanosheet materials	0–2.5	*	*	−20–80 °C	[90]
	$Zn(ClO_4)_2$ -ACN	CCM–I2	0.8–1.4	*	−50.2 °C	-40–25°C	[91]

modifying the solvation structure to lower the freezing point, they can also form stable SEI layers to suppress hydrogen evolution reactions and zinc dendrite growth. The development of high-concentration electrolytes involves exploring novel ion-pair strategies. By introducing asymmetric anions or small organic molecules, the ionic conductivity of the electrolyte can be improved and the freezing point lowered. However, high-concentration electrolytes are more costly and may lead to a reduction in ionic conductivity. Therefore, future research needs to strike a balance between performance and cost. Regarding the innovation of hydrogel electrolytes, constructing multifunctional network structures allows high ionic conductivity and good flexibility even at low temperatures. For example, hydrogel electrolytes composed of sodium alginate, arabic gum, and glycerol still exhibit excellent performance at −20 °C. At the same time, functional groups in hydrogel electrolytes can

interact with zinc ions via electrostatic interactions to form uniform ion conduction channels, improving the reversibility and dendrite resistance of zinc electrodes. Facing the challenges of organic solvent-based non-aqueous electrolytes, solvation capability and safety remain key considerations in design. Future research should focus on developing environmentally friendly organic solvents to reduce environmental impact.

In summary, the future direction should focus on combining multiple strategies, integrating the advantages of additives, high-concentration electrolytes, and hydrogel electrolytes to develop electrolyte systems with a wide temperature range and high safety. Additionally, exploring new materials such as organic solvents with low melting points and high flashpoints, along with optimizing the solvation structure of electrolytes, will further enhance battery performance and safety.

5. Summary and Outlook

Although more and more people are concerned about the problems of ZIBs in extreme environments, the research on ZIBs in these extreme environments still needs to be developed.[23–24] This paper summarizes the challenges faced by ZIBs in extreme environments and the corresponding strategies. We first separately aanalyzed the challenges faced by zinc-ion batteries (ZIBs) in high and low temperature environments. In low temperature environments, issues such as low ionic conductivity, reduced ion migration, salt crystal precipitation, and even electrolyte solidification affect battery performance. In high temperature environments, challenges include water evaporation, electrolyte decomposition, hydrogen evolution reaction (HER), and zinc anodic corrosion. Next, we summarize the design strategies for four types of electrolytes: pure organic electrolytes, electrolyte additives/co-solvents, high-concentration electrolytes, and hydrogel electrolytes. We analyze the principles behind these four electrolytes in improving the extreme temperature performance. Each electrolyte has its own strengths and weaknesses in the scopes of operational range, ionic conductivity, cost, and thermal stability. Some of the published papers are summarized. These research findings hold significant theoretical and practical importance in enhancing the stability of ZIBs at extreme temperature conditions and advancing their practical applications. Specifically, pure organic electrolytes have unique advantages in expanding the operating voltage window, avoiding the hydrogen evolution reaction and side reactions, as well as preventing water evaporation. Organic solvents with high dielectric constants and high boiling points can significantly improve the kinetic and thermodynamic capacity of electrolytes. Additionally, high-flash-point organic solvents can achieve non-flammability at high temperatures. However, they have drawbacks such as high viscosity, slow ion migration, and high cost. Moreover, they require high solubility for zinc metal salts. Finding organic solvents that simultaneously meet high dielectric constants, high boiling points, and high flash points is a challenge, which greatly limits the development of pure organic electrolytes.

In the presence of electrolyte additives/ cosolvents, the excellent thermal stability and low freezing point (T_f) of organic solvents can effectively widen the operating temperature window of the electrolyte. Organic solvents enhance the ion transport properties of the electrolyte and increase the transfer rate of zinc ions. They can form a stable SEI (Solid Electrolyte Interphase) film on the electrode surface, preventing corrosion of the zinc anode under extreme conditions and enhancing the stability of the electrode interface. However, the strategy of electrolyte additives/cosolvents highly depends on the proportion and intrinsic properties of organic solvents in the aqueous solution, and the low ion conductivity of some organic solvents may hinder their application. The performance of electrolyte additives/cosolvents is better at high temperatures; however, the presence of water molecules in the electrolyte still limits their performance at low temperatures. The WIS (Water-in-Salt) strategy can extend the temperature range of the electrolyte, improve ion conductivity, increase ion transfer frequencies, and broaden the electrochemical working window. Nevertheless, WIS electrolytes face challenges such as high viscosity, the relatively high cost of some metal zinc salts, and issues related to crystalline precipitation. Most reported WIS electrolytes use cost-effective $ZnCl_2$, which has high solubility in water (432 g/ 100 ml). High concentrations of salt can disrupt strong hydrogen bonds (HBs) in the electrolyte, lowering the freezing point (T_f). Therefore, the high salt concentration strategy exhibits excellent performance in low-temperature environments. Hydrogel electrolytes, formed by polymerization into a three-dimensional network structure, contain numerous charged functional groups that interact with water molecules in the electrolyte. This disrupts the strong HB network between water molecules, reducing the freezing point (T_f) of the electrolyte. Additionally, hydrogel electrolytes demonstrate outstanding water retention, limiting water molecule evaporation, enhancing the thermal stability of the electrolyte, and enabling hydrogel electrolytes to achieve excellent wide-temperature performance.

Based on these electrolytes, we discuss the reported strategies and parameters. The flash and melting points of commonly used organic solvents for organic electrolytes have remarkable effect on the temperature window of organic electrolytes. Solvents with higher flash points demonstrate better tolerance to temperature variations, thus offering advantages in enhancing the high-temperature performance of the electrolyte. For instance, solvents like TEP, PC, EG and GL exhibit higher flash points. If the flash point of the electrolyte is too low, there is a risk of ignition when the operating temperature reaches the flash point. Melting point, serving as the standard for solid-liquid transition, to some extent, determines the minimum working temperature of the electrolyte. Lower melting point additives play a more substantial role in reducing the electrolyte's T_f. To achieve outstanding performance in low-temperature environments, solvents with low melting points are crucial. For example, solvents like MeOH, DOL and DMF have relatively low melting points, which significantly reduces the Tt. The dielectric constant (ε) is another parameter reflecting the properties of organic solvents. Higher

ε usually means Zn^{2+} and organic solvent between the stronger ion - dipole interaction. Solvents with a moderate dielectric constant are beneficial for the dissolution of metal zinc salts. In addition to these physical properties, further exploration of failure mechanisms under low and high-temperature conditions is required. Common spectroscopic techniques, such as Raman spectroscopy and infrared spectroscopy, can be employed to analyze the coordination environment within the electrolyte. In-situ Raman and in-situ FTIR can be employed to study changes at the electrolyte/electrode interface during cycling. Simulation and computation can also be used to predict and validate potential interface reactions. Finally, we propose some ideas and suggestions for improving the performance of zinc-ion batteries in extreme environments:

1) In the 3D network structure of a hydrogel electrolyte, numerous charged groups are present, allowing for interactions with water molecules within the electrolyte. This property leads to a reduction in the electrolyte's T_f, resulting in excellent performance at low temperatures. However, the majority of hydrogel electrolytes exhibit subpar performance at high temperatures. This limitation can be mitigated by introducing high-flash-point organic solvents into the hydrogel electrolyte, enhancing its thermal stability under elevated temperatures. This approach facilitates the attainment of operational capabilities in both low and high-temperature environments. In the case of highly concentrated salt electrolytes, the solubility of most zinc metal salts is notably low, impeding further development. To address this challenge, the introduction of suitable co-solvents is necessary to augment their solubility
2) Battery separators play a crucial role in preventing short circuits between the positive and negative electrodes and enhancing ion transport pathways. Currently, glass fiber (GF) is commonly used as a separator in zinc-ion battery research. However, GF separators lack ideal mechanical performance and contain large, unevenly distributed internal pores, making them prone to the formation of zinc dendrites and subsequent short circuits. Conventional separators composed of polyethylene (PE) or polypropylene (PP) tend to undergo polymer structure degradation at high temperatures. Additionally, the surface of commercial PE separators lacks polar functional groups, leading to decreased electrolyte wettability, ion conductivity, and lithium-ion transfer rate. Therefore, research on separators is a pivotal aspect influencing the operational performance of ZIBs at extreme temperature environments.
3) Most cathode materials exhibit structural instability in either high or low-temperature environments, leading to structural collapse during cycling processes. Therefore, in addition to ensuring high energy density, the design of the electrolyte must also consider structural stability in high or low-temperature conditions. Achieving high energy density in such environments presents several challenges. Consequently, the development of an artificial solid electrolyte interface (SEI) remains a viable direction for research.

In summary, to meet the demands of ZIBs in both high and low-temperature environments, researchers have developed various electrolytes, achieving significant progress. However, there are still few solutions that can effectively operate in both high and low-temperature conditions. Developing efficient and outstanding batteries for high and low-temperature environments continues to face many challenges. This paper provides an overview primarily focused on strategies for low/high-temperature zinc electrolytes, and it is anticipated that more satisfactory electrolytes will be developed in the future.

Author Contributions

Xingtai Liu wrote the paper with support from Hao Wang, Houzhao Wan. Xiaofang Wang, Chao Xia, Jingying Li, Jia Yao and Lin Lv were responsible for paper revision and literature search; Hao Wang and Houzhao Wan contributed to the funding support.

Acknowledgements

This research was supported by the National Natural Science Foundation of China (No. 52272198 and 52002122).

Conflict of Interests

The authors declare that they have no known competing financial interests or personal relationships that could have appeared to influence the work reported in this paper.

Keywords: Zinc-ion battery · Electrolyte strategy · Extreme Temperature · Thermodynamics · Dynamics

[1] E. Aramendia, P. E. Brockway, P. G. Taylor, J. B. Norman, M. K. Heun, J. Zeke, *Nat. Energy* **2024**, 1–14.
[2] a) A. Innocenti, S. Beringer, S. Passerini, *Nat. Rev. Mater.* **2024**, *9*, 347–357; b) J. Hao, X. Feng, X. Chen, X. Jin, X. Wang, T. Hao, F. Hong, X. J. A. E. Du, *Appl. Energy* **2024**, *373*, 123974.
[3] a) R. Yao, Y. Zhao, L. Wang, C. Xiao, F. Kang, C. Zhi, C. J. E. Yang, *E. Science* **2024**, *17*, 3112–3122; b) Z. Wu, J. Yao, C. Chen, X. Chen, X. Pan, J. Zheng, Y. Gan, J. Li, X. Liu, C. Xia, *Chem. Eng. J.* **2024**, *479*, 147889.
[4] a) S. Zhan, Y. Guo, K. Wu, F. Ning, X. Liu, Y. Liu, Q. Li, J. Zhang, S. Lu, J. J. Yi, *Chem. Eur. J.* **2024**, *30*, e202303211; b) K. Wu, X. Liu, F. Ning, S. Subhan, Y. Xie, S. Lu, Y. Xia, J. Yi, *ChemSusChem* **2024**, e202401251; c) H. Zhang, F. Ning, Y. Guo, S. Subhan, X. Liu, S. Shi, S. Lu, Y. Xia, J. Yi, *ACS Energy Lett.* **2024**, *9*, 4761–4784.
[5] a) J. Yao, B. Zhang, X. Wang, L. Tao, J. Ji, Z. Wu, X. Liu, J. Li, Y. Gan, J. J. Zheng, *Angew. Chem. Int. Ed.* **2024**, 619–629, e202409986; b) J. Zhang, S. Lu, J. Yi, *Nano-Micro Lett.* **2024**.
[6] a) Q. Fu, S. Hao, X. Zhang, H. Zhao, F. Xu, J. Yang, *Energy Environ. Sci.* **2023**, *16*, 1291–1311; b) C.-Y. Wang, T. Liu, X.-G. Yang, S. Ge, N. V. Stanley, E. S. Rountree, Y. Leng, B. D. McCarthy, *Nature* **2022**, *611*, 485–490; c) S. Liu, R. Zhang, J. Mao, Y. Zhao, Q. Cai, Z. Guo, *Sci. Adv.* **2022**, *8*, eabn5097; d) Z. Li, Y. Xu, L. Wu, Y. An, Y. Sun, T. Meng, H. Dou, Y. Xuan, X. Zhang, *Nat. Commun.* **2022**, *13*, 132.
[7] R. Zhang, W. K. Pang, J. P. Vongsvivut, J. A. Yuwono, G. Li, Y. Lyu, Y. Fan, Y. Zhao, S. Zhang, J. J. E. Mao, *Science* **2024**.
[8] a) Y. Wang, T. Wang, S. Bu, J. Zhu, Y. Wang, R. Zhang, H. Hong, W. Zhang, J. Fan, C. Zhi, *Nat. Commun.* **2023**, *14*, 1828; b) Y. Wang, Z. Wang, W. K. Pang, W. Lie, J. A. Yuwono, G. Liang, S. Liu, A. M. D. Angelo, J. Deng, Y. Fan, *Nat. Commun.* **2023**, *14*, 2720; c) Y. Zhao, Y. Lu, H. Li, Y.

Zhu, Y. Meng, N. Li, D. Wang, F. Jiang, F. Mo, C. Long, *Nat. Commun.* **2022**, *13*, 752.
[9] H. Ren, S. Li, B. Wang, Y. Zhang, T. Wang, Q. Lv, X. Zhang, L. Wang, X. Han, F. Jin, *Adv. Mater.* **2023**, *35*, 2208237.
[10] M. Wu, X. Wang, F. Zhang, Q. Xiang, Y. Li, J. J. E. Guo, *E. Science* **2024**, *17*, 619–629.
[11] a) Y. Geng, L. Pan, Z. Peng, Z. Sun, H. Lin, C. Mao, L. Wang, L. Dai, H. Liu, K. Pan, *Energy Storage Mater.* **2022**; b) J. Zhu, M. Yang, Y. Hu, M. Yao, J. Chen, Z. Niu, *Adv. Mater.* **2023**, 2304426; c) X. Li, X. Wang, L. Ma, W. Huang, *Adv. Energy Mater.* **2022**, *12*, 2202068.
[12] L. Sun, Z. Song, C. Deng, Q. Wang, F. Mo, H. Hu, G. Liang, *Batteries* **2023**, *9*, 386.
[13] Y. Cui, R. Zhang, S. Yang, L. Liu, S. Chen, *Materials Futures* **2023**.
[14] R. Katiyar, P. J. C. P. Sappidi, *J. Chem. Phys.* **2024**, *587*, 112424.
[15] a) S. Al Hallaj, J. Prakash, J. Selman, *J. Power Sources* **2000**, *87*, 186–194; b) J. Jiang, H. Ruan, B. Sun, W. Zhang, W. Gao, L. Zhang, *Appl. Energy* **2016**, *177*, 804–816; c) C. Zhang, J. Jiang, Y. Gao, W. Zhang, Q. Liu, X. Hu, *Appl. Energy* **2017**, *194*, 569–577.
[16] a) J. Liu, W. Zhou, R. Zhao, Z. Yang, W. Li, D. Chao, S.-Z. Qiao, D. Zhao, *J. Am. Chem. Soc.* **2021**, *143*, 15475–15489; b) J. Wang, Q. Zhu, F. Li, J. Chen, H. Yuan, Y. Li, P. Hu, M. S. Kurbanov, H. Wang, *Chem. Eng. J.* **2022**, *433*, 134589.
[17] N. Piao, X. Gao, H. Yang, Z. Guo, G. Hu, H.-M. Cheng, F. Li, *eTransportation* **2022**, *11*, 100145.
[18] a) D. J. Noelle, M. Wang, A. V. Le, Y. Shi, Y. Qiao, *Appl. Energy* **2018**, *212*, 796–808; b) L. Wang, H. Yu, D. Chen, Y. Jin, L. Jiang, H. He, G. Zhou, Z. Xie, *Carbon Neutralization* **2024**, *3*, 996–1008.
[19] a) Y. Wang, H. Wei, Z. Li, X. Zhang, Z. Wei, K. Sun, H. Li, *The Chemical Record* **2022**, *22*, e202200132; b) J. Wan, R. Wang, Z. Liu, S. Zhang, J. Hao, J. Mao, H. Li, D. Chao, L. Zhang, C. Zhang, *Adv. Mater.* **2024**, *36*, 2310623.
[20] a) J. Zheng, P. Shi, C. Chen, X. Chen, Y. Gan, J. Li, J. Yao, Y. Yang, L. Lv, G. Ma, *Sci. China Mater.* **2023**, *66*, 3113–3122; b) J. Ji, H. Wan, B. Zhang, C. Wang, Y. Gan, Q. Tan, N. Wang, J. Yao, Z. Zheng, P. J. A. E. M. Liang, *Adv. Energy Mater.* **2021**, *11*, 2003203.
[21] a) N. Patil, C. de la Cruz, D. Ciurduc, A. Mavrandonakis, J. Palma, R. Marcilla, *Adv. Energy Mater.* **2021**, *11*, 2100939; b) J. Li, K. Xu, J. Yao, Y. Yang, Z. Wu, J. Zhang, X. Chen, J. Zheng, Y. Yang, X. Liu, *Energy Storage Mater.* **2024**, 103844.
[22] a) Z. Chen, T. Wang, Y. Hou, Y. Wang, Z. Huang, H. Cui, J. Fan, Z. Pei, C. Zhi, *Adv. Mater.* **2022**, *34*, 2207682; b) M. Zhao, Y. Lv, S. Zhao, Y. Xiao, J. Niu, Q. Yang, J. Qiu, F. Wang, S. Chen, *Adv. Mater.* **2022**, *34*, 2206239.
[23] Z. Wu, J. J. B. Liu, *Supercaps* e202400483.
[24] M. Chen, S. Xie, X. Zhao, W. Zhou, Y. Li, J. Zhang, Z. Chen, D. Chao, *Energy Storage Mater.* **2022**, *51*, 683–718.
[25] J. Qu, Z. Jiang, J. Zhang, *J. Energy Storage* **2022**, *52*, 104811.
[26] a) Y. Yan, S. Duan, B. Liu, S. Wu, Y. Alsaid, B. Yao, S. Nandi, Y. Du, T. W. Wang, Y. Li, *Adv. Mater.* **2023**, *35*, 2211673; b) X. Zhu, C. Ji, Q. Meng, H. Mi, Q. Yang, Z. Li, N. Yang, J. Qiu, *Small* **2022**, *18*, 2200055; c) W. Deng, Z. Xu, X. Wang, *Energy Storage Mater.* **2022**, *52*, 52–60; d) X. Gong, Z. Zhang, Z. Zhang, J. Dai, X. Li, B. J. B. Wang, *Supercaps* **2024**, *7*, e202400095.
[27] a) P. Xiong, Y. Kang, N. Yao, X. Chen, H. Mao, W.-S. Jang, D. M. Halat, Z.-H. Fu, M.-H. Jung, H. Y. Jeong, *ACS Energy Lett.* **2023**, *8*, 1613–1625; b) Y. Ma, Q. Zhang, L. Liu, Y. Li, H. Li, Z. Yan, J. Chen, *Natl. Sci. Rev.* **2022**, *9*, nwac051; c) X. Liu, X. Wang, J. Yao, J. Li, Y. Gan, Z. Wu, J. Zheng, W. Hao, L. Lv, *Adv. Energy Mater.* **2024**, 2400090.
[28] a) P. Chen, X. Sun, T. Pietsch, B. Plietker, E. Brunner, M. Ruck, *Adv. Mater.* **2023**, *35*, 2207131; b) J. Zheng, B. Zhang, X. Chen, W. Hao, J. Yao, J. Li, Y. Gan, X. Wang, X. Liu, Z. Wu, *J. Am. Chem. Soc.* **2024**, *16*, 145.
[29] a) C. Cui, D. Han, H. Lu, Z. Li, K. Zhang, B. Zhang, X. Guo, R. Sun, X. Ye, J. Gao, *Adv. Energy Mater.* **2023**, *13*, 2301466; b) J. Wang, Y. Huang, B. Liu, Z. Li, J. Zhang, G. Yang, P. Hiralal, S. Jin, H. Zhou, *Energy Storage Mater.* **2021**, *41*, 599–605.
[30] S. J. Zhang, J. Hao, Y. Zhu, H. Li, Z. Lin, S. Z. Qiao, *Angew. Chem.* **2023**, *135*, e202301570.
[31] M. Li, R. P. Hicks, Z. Chen, C. Luo, J. Guo, C. Wang, Y. Xu, *Chem. Rev.* **2023**, *123*, 1712–1773.
[32] a) X. Gao, J. Yang, Z. Xu, Y. Nuli, J. Wang, *Energy Storage Mater.* **2023**, *54*, 382–402; b) T. Nguyen Thanh Tran, M. Zhao, S. Geng, D. G. Ivey, *Batteries & Supercaps* **2022**, *5*, e202100420.
[33] B. Wang, R. Zheng, W. Yang, C. Hou, Q. Zhang, K. Li, Y. Li, H. Wang, *Available at SSRN 4510401*.
[34] C. Xie, S. Liu, H. Wu, Q. Zhang, C. Hu, Z. Yang, H. Li, Y. Tang, H. Wang, *Sci. Bull.* **2023**.
[35] a) L. Deng, K. Goh, F.-D. Yu, Y. Xia, Y.-S. Jiang, W. Ke, Y. Han, L.-F. Que, J. Zhou, Z.-B. Wang, *Energy Storage Mater.* **2022**, *44*, 82–92; b) B. Wu, Y. Mu, Z. Li, M. Li, L. Zeng, T. Zhao, *Chin. Chem. Lett.* **2023**, *34*, 107629; c) Y. Yang, S. Yao, Z. Liang, Y. Wen, Z. Liu, Y. Wu, J. Liu, M. Zhu, *ACS Energy Lett.* **2022**, *7*, 885–896.
[36] X. Shi, Y. Zhong, Y. Yang, J. Zhou, X. Cao, S. Liang, *Angew. Chem. Int. Ed.* e202414777.
[37] a) N. Wang, X. Chen, H. Wan, B. Zhang, K. Guan, J. Yao, J. Ji, J. Li, Y. Gan, L. Lv, *Adv. Funct. Mater.* **2023**, *33*, 2300795; b) X. Ai, Q. Zhao, Y. Duan, Z. Chen, Z. Zhang, Y. Liu, Y. Gao, *Cell Rep. Phys. Sci.* **2022**, *3*; c) H. Chang, Z.-Y. Luo, X.-R. Shi, X.-X. Caos.-q., J. Liang, *T Nonferr Metal Soc.* **2024**, *34*, 3358–3371.
[38] a) H. Peng, Y. Fang, J. Wang, P. Ruan, Y. Tang, B. Lu, X. Cao, S. Liang, *J. Zhou, Mater.* **2022**, *5*, 4363–4378; b) J. Chen, H. Chang, Z. Liu, Z. Chen, S. Han, X. Cao, S. Liang, *J. Power Sources.* **2024**, *613*, 234904.
[39] a) P. V. Chombo, Y. Laoonual, *J. Power Sources* **2020**, *478*, 228649; b) Y. Quan, M. Yang, M. Chen, W. Zhou, X. Han, J. Chen, B. Liu, S. Shi, P. Zhang, *Chem. Eng. J.* **2023**, *458*, 141392.
[40] W. Xu, J. Li, X. Liao, L. Zhang, X. Zhang, C. Liu, K. Amine, K. Zhao, J. Lu, *J. Am. Chem. Soc.* **2023**, *145*, 22456–22465.
[41] a) H. Ren, S. Li, B. Wang, Y. Zhang, T. Wang, Q. Lv, X. Zhang, L. Wang, X. Han, F. Jin, C. Bao, P. Yan, N. Zhang, D. Wang, T. Cheng, H. Liu, S. Dou, *Adv. Mater.* **2022**, *35*; b) R. Yao, L. Qian, G. Zhao, H. Zhu, T. Qin, C. Xiao, H. Lin, F. Kang, C. Zhi, C. Yang, *J. Mater. Chem. A.* **2023**, *11*, 1361–1368.
[42] a) T. C. Li, Y. Lim, X. L. Li, S. Luo, C. Lin, D. Fang, S. Xia, Y. Wang, H. Y. Yang, *Adv. Energy Mater.* **2022**, *12*, 2103231; b) H. Yan, X. Zhang, Z. Yang, M. Xia, C. Xu, Y. Liu, H. Yu, L. Zhang, J. Shu, *Coord. Chem. Rev.* **2022**, *452*, 214297.
[43] P. Xiong, Y. Kang, N. Yao, X. Chen, H. Mao, W.-S. Jang, D. M. Halat, Z.-H. Fu, M.-H. Jung, H. Y. Jeong, Y.-M. Kim, J. A. Reimer, Q. Zhang, H. S. Park, *ACS Energy Lett.* **2023**, *8*, 1613–1625.
[44] Y. Quan, W. Zhou, T. Wu, M. Chen, X. Han, Q. Tian, J. Xu, J. Chen, *Chem. Eng. J.* **2022**, *446*, 137056.
[45] Y. Lv, Y. Xiao, L. Ma, C. Zhi, S. Chen, *Adv. Mater.* **2022**, *34*, 2106409.
[46] a) T. Sun, S. Zheng, H. Du, Z. Tao, *Nano-Micro Lett.* **2021**, *13*, 1–10; b) X. L. Wang, J. P. Xue, X. P. Sun, Y. X. Zhao, S. Q. Wu, Z. S. Yao, J. Tao, *Chem. Eur. J.* **2020**, *26*, 6778–6783.
[47] Q. Zhang, Y. Ma, Y. Lu, L. Li, F. Wan, K. Zhang, J. Chen, *Nat. Commun.* **2020**, *11*.
[48] T. Sun, X. Yuan, K. Wang, S. Zheng, J. Shi, Q. Zhang, W. Cai, J. Liang, Z. Tao, *JJ. Mater. Chem. A.* **2021**, *9*, 7042–7047.
[49] a) X. Wang, Y. Ying, X. Li, S. Chen, G. Gao, H. Huang, L. Ma, *Energy Environ. Sci.* **2023**, *16*, 4572–4583; b) Y. Xie, X. Ding, J. Wang, G. Ye, *Angew. Chem. Int. Ed.* **2023**, e202313951.
[50] F. Mo, G. Liang, Q. Meng, Z. Liu, H. Li, J. Fan, C. Zhi, *Energy Environ. Sci.* **2019**, *12*, 706–715.
[51] Y. Shi, R. Wang, S. Bi, M. Yang, L. Liu, Z. Niu, *Adv. Funct. Mater.* **2023**, *33*, 2214546.
[52] S. He, Q. Cheng, Y. Liu, Q. Rong, M. Liu, *Sci. China Mater.* **2022**, *65*, 1980–1986.
[53] J. L. Yang, T. Xiao, T. Xiao, J. Li, Z. Yu, K. Liu, P. Yang, H. Fan, *Adv. Mater.* **2024**, 2313610.
[54] C. D. Lorenz, C.-M. Hsieh, C. A. Dreiss, M. Lawrence, *Langmuir.* **2011**, *27*, 546–553.
[55] F. Huang, Y. Guo, W. Zhao, R. Wu, Y. Dong, G. Long, P. Du, *Chem. Eng. J.* **2024**, 155248.
[56] M. Chen, J. Chen, W. Zhou, X. Han, Y. Yao, C. P. Wong, *Adv. Mater.* **2021**, *33*, 2007559.
[57] S. Huang, L. Hou, T. Li, Y. Jiao, P. Wu, *Adv. Mater.* **2022**, *34*, 2110140.
[58] X. Li, D. Wang, F. Ran, *Energy Storage Mater.* **2023**, *56*, 351–393.
[59] Y. Li, J. Yuan, Y. Qiao, H. Xu, Z. Zhang, W. Zhang, G. He, H. Chen, *Dalton Trans.* **2023**.
[60] a) X. Li, A. Wu, J. Li, Z. Li, D. Lee, S. W. Lee, *ACS Energy Lett.* **2023**, *8*, 4061–4068; b) L. Sun, Z. Song, C. Deng, Q. Wang, F. Mo, H. Hu, G. Liang, *Batteries* **2023**, *9*, 386.
[61] N. Wang, X. Dong, B. Wang, Z. Guo, Z. Wang, R. Wang, X. Qiu, Y. Wang, *Angew. Chem. Int. Ed.* **2020**, *59*, 14577–14583.
[62] X. Qiu, N. Wang, X. Dong, J. Xu, K. Zhou, W. Li, Y. Wang, *Angew. Chem. Int. Ed.* **2021**, *133*, 21193–21200.
[63] Z. Chen, Y. Tang, X. Du, B. Chen, G. Lu, X. Han, Y. Zhang, W. Yang, P. Han, J. Zhao, *Angew. Chem. Int. Ed.* **2020**, *59*, 21769–21777.
[64] H. Du, X. Qi, L. Qie, Y. Huang, *Adv. Funct. Mater.* **2023**, 2302546.
[65] a) J. Guo, Y. Chen, Y. Xiao, C. Xi, G. Xu, B. Li, C. Yang, Y. Yu, *Chem. Eng. J.* **2021**, *422*, 130526; b) S.-J. Tan, J. Yue, Y.-F. Tian, Q. Ma, J. Wan, Y. Xiao, J. Zhang, Y.-X. Yin, R. Wen, S. Xin, *Energy Storage Mater.* **2021**, *39*, 186–

193; c) H. Yang, C. Guo, J. Chen, A. Naveed, J. Yang, Y. Nuli, J. Wang, *Angew. Chem. Int. Ed.* **2019**, *58*, 791–795.
[66] Y. Chen, S. He, Q. Rong, *J. Energy Storage.* **2023**, *73*, 109023.
[67] C. Cui, D. Han, H. Lu, Z. Li, K. Zhang, B. Zhang, X. Guo, R. Sun, X. Ye, J. Gao, *Adv. Energy Mater.* **2023**, *13*, 2301466.
[68] B. Wang, R. Zheng, W. Yang, C. Hou, Q. Zhang, K. Li, Y. Li, H. Wang, *ACS Appl. Energ. Mater.* **2023**, *6*, 12249–12258.
[69] C. Xie, S. Liu, H. Wu, Q. Zhang, C. Hu, Z. Yang, H. Li, Y. Tang, H. Wang, *Sci. Bull.* **2023**, *68*, 1531–1539.
[70] Y. Dong, N. Zhang, Z. Wang, J. Li, Y. Ni, H. Hu, F. Cheng, *J. Energy Chem.* **2023**, *83*, 324–332.
[71] P. Xiong, Y. Kang, N. Yao, X. Chen, H. Mao, W.-S. Jang, D. M. Halat, Z.-H. Fu, M.-H. Jung, H. Jeong, *ACS Energy Lett.* **2023**, *8*, 1613–1625.
[72] L. Yu, J. Huang, S. Wang, L. Qi, S. Wang, C. Chen, *Adv. Mater.* **2023**, *35*, 2210789.
[73] D. Han, C. Cui, K. Zhang, Z. Wang, J. Gao, Y. Guo, Z. Zhang, S. Wu, L. Yin, Z. Weng, *Nat. Sustain.* **2022**, *5*, 205–213.
[74] H. Du, K. Wang, T. Sun, J. Shi, X. Zhou, W. Cai, Z Tao, *Chem. Eng. J.* **2022**, *427*, 131705.
[75] T. Sun, X. Yuan, K. Wang, S. Zheng, J. Shi, Q. Zhang, W. Cai, J. Liang, Z. Tao, *J. Mater. Chem. A.* **2021**, *9*, 7042–7047.
[76] Q. Zhang, Y. Ma, Y. Lu, L. Li, F. Wan, K. Zhang, J. Chen, *Nat. Commun.* **2020**, *11*, 4463.
[77] G. Yang, J. Huang, X. Wan, B. Liu, Y. Zhu, J. Wang, O. Fontaine, S. Luo, P. Hiralal, Y. Guo, *EcoMat.* **2022**, *4*, e12165.
[78] N. Patil, C. de la Cruz, D. Ciurduc, A. Mavrandonakis, J. Palma, R. Marcilla, *Adv. Energy Mater.* **2021**, *11*, 2100939.
[79] L. Cao, D. Li, F. A. Soto, V. Ponce, B. Zhang, L. Ma, T. Deng, J. M. Seminario, E. Hu, X. Yang, *Angew. Chem. Int. Ed.* **2021**, *60*, 18845–18851.
[80] Y. Pu, C. Wang, J. Feng, Y. Xu, K. Su, B. Yang, G. Tian, J. Lang, *J. Power Sources.* **2023**, *571*, 233061.
[81] Y. Shi, R. Wang, S. Bi, M. Yang, L. Liu, Z. Niu, *Adv. Funct. Mater.* **2023**, *33*, 2214546.
[82] S. Zhao, K. Wang, S. Tang, X. Liu, K. Peng, Y. Xiao, Y. J. Chen, *Energy Technol.* **2020**, *8*, 1901229.
[83] X. Li, H. Wang, X. Sun, J. Li, Y. Liu, *ACS Appl. Energ. Mater.* **2021**, *4*, 12718–12727.
[84] W. Deng, Z. Zhou, Y. Li, M. Zhang, X. Yuan, J. Hu, Z. Li, C. Li, R. Li, *ACS Nano* **2020**, *14*, 15776–15785.
[85] Y. Wu, Y. Deng, K. Zhang, Y. Wang, L. Wang, L. Yan, *J. Mater. Chem. A.* **2022**, *10*, 17721–17729.
[86] J. Wu, Y. Wang, D. Deng, Y. Bai, M. Liu, X. Zhao, X. Xiong, Y. Lei, *J. Mater. Chem. A.* **2022**, *10*, 19304–19319.
[87] Z. Chen, Y. Tang, X. Du, B. Chen, G. Lu, X. Han, Y. Zhang, W. Yang, P. Han, J. E. Zhao, *Angew. Chem. Int. Ed.* **2020**, *59*, 21769–21777.
[88] N. Wang, X. Dong, B. Wang, Z. Guo, Z. Wang, R. Wang, X. Qiu, Y. Wang, *Angew. Chem. Int. Ed.* **2020**, *59*, 14577–14583.
[89] X. Qiu, N. Wang, X. Dong, J. Xu, K. Zhou, W. Li, Y. Wang, *Angew. Chem. Int. Ed.* **2021**, *133*, 21193–21200.
[90] S. Li, Q. Tian, J. Chen, Y. Chen, P. Guo, C. Wei, P. Cui, J. Jiang, X. Li, Q. Xu, *Chem. Eng. J.* **2023**, *457*, 141265.
[91] C. Song, Z. Gong, C. Bai, F. Cai, Z. Yuan, X. Liu, *Nano Res.* **2022**, 1–8.
[92] a) H. Du, K. Wang, T. Sun, J. Shi, X. Zhou, W. Cai, Z. Tao, *Chem. Eng. J.* **2022**, *427*, 131705; b) A. Wang, W. Zhou, A. Huang, M. Chen, Q. Tian, J. Chen, *J. Colloid Interface Sci.* **2021**, *586*, 362–370; c) J. Zhou, H. Yuan, J. Li, W. Wei, Y. Li, J. Wang, L. Cheng, D. Zhang, Y. Ding, D. Chen, *Chem. Eng. J.* **2022**, *442*, 136218; d) B. Qiu, L. Xie, G. Zhang, K. Cheng, Z. Lin, W. Liu, C. He, P. Zhang, H. Mi, *Chem. Eng. J.* **2022**, *449*, 137843; e) Y. Dong, N. Zhang, Z. Wang, J. Li, Y. Ni, H. Hu, F. Cheng, *J. Energy Chem.* **2023**; f) R. Qin, Y. Wang, M. Zhang, Y. Wang, S. Ding, A. Song, H. Yi, L. Yang, Y. Song, Y. Cui, *Nano Energy* **2021**, *80*, 105478; g) N. Wang, Y. Yang, X. Qiu, X. Dong, Y. Wang, Y. Xia, *ChemSusChem* **2020**, *13*, 5556–5564; h) N. Chang, T. Li, R. Li, S. Wang, Y. Yin, H. Zhang, X. Li, *Energy Environ. Sci.* **2020**, *13*, 3527–3535; i) F. Ming, Y. Zhu, G. Huang, A.-H. Emwas, H. Liang, Y. Cui, H. N. Alshareef, *J. Am. Chem. Soc.* **2022**, *144*, 7160–7170; j) L. Yu, J. Huang, S. Wang, L. Qi, S. Wang, C. Chen, *Adv. Mater.* **2023**, 2210789; k) D. Han, C. Cui, K. Zhang, Z. Wang, J. Gao, Y. Guo, Z. Zhang, S. Wu, L. Yin, Z. Weng, *Nat. Sustain.* **2022**, *5*, 205–213; l) X. Li, H. Wang, X. Sun, J. Li, Y.-N. Liu, *ACS Appl. Energ. Mater.* **2021**, *4*, 12718–12727; m) W. Yang, X. Du, J. Zhao, Z. Chen, J. Li, J. Xie, Y. Zhang, Z. Cui, Q. Kong, Z. Zhao, *Joule* **2020**, *4*, 1557–1574; n) S. Li, Q. Tian, J. Chen, Y. Chen, P. Guo, C. Wei, P. Cui, J. Jiang, X. Li, Q. Xu, *Chem. Eng. J.* **2023**, *457*, 141265; o) Z. Chen, T. Liu, Z. Zhao, Z. Zhang, X. Han, P. Han, J. Li, J. Wang, J. Li, S. Huang, *J. Power Sources* **2020**, *457*, 227994; p) X. Lin, G. Zhou, M. J. Robson, J. Yu, S. C. Kwok, F. Ciucci, *Adv. Funct. Mater.* **2022**, *32*, 2109322; q) Y. Wang, Y. Chen, *Electrochim. Acta* **2021**, *395*, 139178; r) H. Wang, W. Wei, X. Liu, S. Xu, Y. Dong, R. He, *Energy Storage Mater.* **2023**, *55*, 597–605; s) H. Wang, X. Li, D. Jiang, S. Wu, W. Yi, X. Sun, J. Li, *J. Power Sources* **2022**, *528*, 231210; t) H. Yang, J. Zhang, J. Yao, D. Zuo, J. Xu, H. Zhang, *J. Power Sources* **2022**, *548*, 232070; u) C. Jia, X. Zhang, S. Liang, Y. Fu, W. Liu, J. Chen, X. Liu, L. Zhang, *J. Power Sources* **2022**, *548*, 232072; v) T. Wei, Y. Ren, Z. Li, X. Zhang, D. Ji, L. Hu, *Chem. Eng. J.* **2022**, *434*, 134646; w) X. Ou, Q. Liu, J. Pan, L. Li, Y. Hu, Y. Zhou, F. Yan, *Chem. Eng. J.* **2022**, *435*, 135051.

Manuscript received: December 22, 2024
Revised manuscript received: January 24, 2025
Accepted manuscript online: February 1, 2025
Version of record online: February 14, 2025